Experimental Assessment on Performance of a Heat Pump Cycle Using R32/R1234yf and R744/R32/R1234yf

Sho Fukuda
Kyushu Univ., Japan, fukuda@phase.cm.kyushu-u.ac.jp

Hedeki Kojima
Kyushu Univ., Japan, kojima@phase.cm.kyushu-u.ac.jp

Chieko Kondou
Nagasaki Univ., Japan, ckondou@nagasaki-u.ac.jp

Nobuo Takata
Kyushu Univ., Japan, takata@cm.kyushu-u.ac.jp

Shigeru Koyama
Kyushu Univ., Japan, koyama@cm.kyushu-u.ac.jp

Experimental Assessment on Performance of a Heat Pump Cycle Using R32/R1234yf and R744/R32/R1234yf

Sho FUKUDA[1]*, Hideki KOJIMA[2], Chieko KONDOU[3], Nobuo TAKATA[2], and Shigeru KOYAMA[1,4]

[1] Faculty of Engineering Sciences, Kyushu University
Kasuga, Fukuoka, 816-8580, Japan
Phone: +81-92-583-7269, Fax: +81-92-583-7833, E-mail: fukuda@phase.cm.kyushu-u.ac.jp

[2] Interdisciplinary Graduate School of Engineering Sciences, Kyushu University
Kasuga, Fukuoka, 816-8580, Japan

[3] Graduate School of Engineering, Nagasaki University
Bunkyo-machi, Nagasaki, 852-8521, Japan

[4] International Institute for Carbon-Neutral Energy Research, Kyushu University
Motooka, Nishi-ku, Fukuoka 819-0395, Japan

ABSTRACT

This study measures the COPs of R744/R32/R1234yf and R32/R1234yf with GWPs of approximately 300 and 200 under two heating modes in experimentally and analytically, where the heat sink water change temperature 10 K and 25 K. In experiment, *COP* of Ternary 300 and Binary 300 are comparable to that of R410A. In analysis, *COP* of Ternary 300, Binary 300 and Binary 200 are higher than that of R410A. Even if temperature glide of zeotropic mixture equal to water temperature change in the heat exchanger, irreversible loss in heat exchanger increases because of lower heat transfer performance of heat exchanger. COP of Ternary 300, Binary 300 and Binary 200 are higher than that of R410A in experiment if compressor is improved and the diameter of connecting pipe and heat exchanger is increased.

1. INTRODUCTION

Hydro-fluorocarbons (HFCs) are widely used as refrigerants in air-conditioning and refrigeration systems. At the 1997 Kyoto Conference (COP3), it was determined that the product and use of HFCs should be regulated due to their high global warming potential (GWP). Therefore, several studies related to Hydro-fluoro-olefins (HFOs) have been reported in the past decade. In the above mentioned situation for the air-conditioning and refrigeration systems, recently, R1234yf is nominated as one of the alternates of HFCs, due to its extremely low GWP. The heating capacity of heat pump cycles using R1234yf is, however, expected to be lower than that of R410A currently most used, because of its lower vapor density and latent heat. To achieve performance equal to R410A, much larger unit is required. In the previous studies (Kojima *et al*., 2015), drop-in experiments on heat pump cycle using mixtures of R1234yf/R32 was carried out; R32 was selected as the second component to increase vapor density and latent heat. It was found that mixtures of R1234yf/R32 were strong candidates for replacing R410A. In this study, adding, to reduce GWP furthermore as maintaining the volumetric capacity, adding R744 to R-32/1234ze(E) was therefore attempted.

On other hand, the mixtures of R744/R32/R1234yf and R32/R1234yf are zeotropic and have a temperature change during the phase-change, typically called temperature glide. When the temperature glide is utilized effectively, the irreversible loss or exergy loss in heat exchangers is reduced and the cycle performance is improved (e.g., Jakobs and Kruse, 1978, Kruse, 1981, McLinden and Radermacher, 1987, Swinney *et al*., 1998). The temperature glide is determined by the composition and pressure of refrigerant mixture.

In this study, the cycle performance of the binary mixture R32/R1234yf and the ternary mixture R744/R32/R1234yf are experimentally compared for their compositions corresponding to GWP of 200 and 300. Additionally, to understand the feasibility of zeotropic refrigerant, irreversible losses in each element are discussed on the experimental data that changing heat sink water temperature of condensation inlet and outlet

2. EXPERIMENTAL SETUP AND METHOD

2.1 Experimental Setup

Figure 1 shows an experimental apparatus, which is a water heat source vapor compression cycle. The experimental apparatus consists of three loops of refrigerant, and cooling and heating water. The refrigerant loop is composed of a manually controlled hermetic type rotary compressor, an oil separator, a condenser, a liquid receiver, a solenoid expansion valve and an evaporator. Using constant-temperature bathes, certain temperature cooling and heating water are supplied to the condenser and the evaporator. Four mixing chambers are installed between each component in the refrigerant loop for measuring the pressure and the bulk mean temperature of refrigerant. The other four mixing chambers are installed in water loops for measuring bulk mean temperatures of water. The dimensions of the condenser and the evaporator are specified in Table 1. Those heat exchangers are both 7200 mm long counter flow double-tube type coils. The refrigerant flows in the inner micro-fin tube, while the water simulating cooling or heating load flows the annulus. Circulating subcooled liquid is sampled at the inlet of expansion valve and the mass fractions of each component are measured by the gas chromatography.

2.2 Experimental Method

2.1.1 Test conditions: Table 2 lists the experimental conditions at heating mode 1 and heating mode 2. The degree of superheat at evaporator outlet is fixed at 3 K for entire experimental conditions. For heating mode 1, water temperatures are fixed as follows. At condenser inlet and outlet, they are kept at 293.15 K and 303.15 K, respectively. At evaporator inlet and outlet, they are kept at 288.15 K and 282.15 K, respectively. Similarly, for heating mode 2, water temperatures at condenser inlet and outlet are kept at 293.15 K to 318.15 K, respectively, and water temperatures at evaporator inlet and outlet are kept at 288.15 K and 282.15 K, respectively. In two heating modes, the heating load is 2.2 kW.

2.2.2 Test refrigerants: Table 3 lists the test refrigerants and their properties: GWP of a 100 year time horizon, normal boiling point, temperature glide at average temperature of 308.15 K, and volumetric capacity defined as the product of latent heat and saturated vapor density. The compositions of the ternary mixtures R744/R32/R1234yf

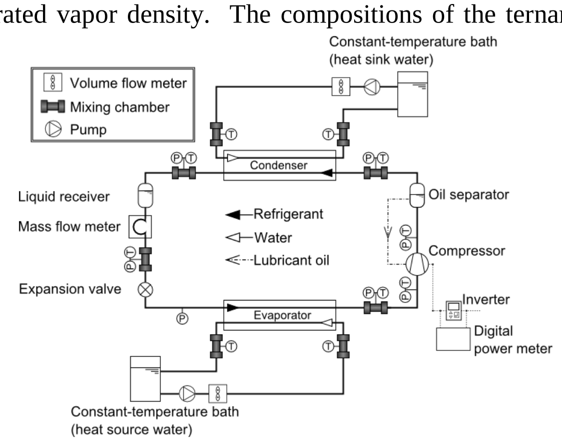

Figure 1: Schematic view of experimental apparatus

Table 1: Specifications of the heat exchangers

	Outside diameter [mm]	Inside diameter [mm]	Length [mm]	Type of tube
		Condenser		
Outer tube	15.88	13.88	7200	Smooth tube
Inner tube	9.53	7.53	7200	Micro-fin tube
		Evaporator		
Outer tube	15.88	13.88	7200	Smooth tube
Inner tube	9.53	7.53	7200	Micro-fin tube

Table 2: Experimental conditions

	Heating mode 1	Heating mode 2
Heat source temperature [K]	288.15→ 282.15 (ΔT = 6 K)	
Heat sink temperature [K]	293.15→303.15 (ΔT = 10 K)	293.15→318.15 (ΔT = 25 K)
Degree of superheat [K]	3	
Heat transfer rate [kW] (Heating/cooling heat load)	2.2	

Table 3: Comparison of properties between test refrigerants

designation	composition (mass%)		GWP_{100}	NBP	Temp. glide *	vol. capacity *
				[K]	[K]	[MJ·m^{-3}]
(Ternary300)	R744/R32/ R1234yf	4/44/52	298	222.30	6.7	14.00
(Ternary200)		5/28/67	190	223.99	10.6	13.03
(Binary300)	R32/ R1234yf	43/57	292	226.55	4.0	12.56
(Binary200)		28/72	190	229.74	6.2	11.21
	R410A		2088	221.74	0.1	15.04

*Bulk temperature 308.15 K

and binary mixtures R32/R1234yf are determined from the criteria at GWP_{100} of 200 and 300.

2.3 Data reduction

The heating load, namely, the heat transfer rates in the condenser is calculated from the refrigerant-side heat balance, as follows:

$$Q_{\mathrm{COND}} = m_{\mathrm{ref}}\left(h_{\mathrm{COND,in}} - h_{\mathrm{COND,out}}\right) \tag{1}$$

The heat transfer rate Q_{COND} corresponds to the capacities or the heat loads of the heating mode operations. The deviation of those heat loads was confirmed to be within 5 %. *COP* of heating modes, COP_{h} is obtained from the above heat load and the compression work, W_{COMPR}, which is found from the specific enthalpy difference between the compressor suction and discharge.

$$COP_{\mathrm{h}} = \frac{Q_{\mathrm{COND}}}{W_{\mathrm{COMPR}}} = \frac{h_{\mathrm{COND,in}} - h_{\mathrm{COND,out}}}{h_{\mathrm{COMPR,out}} - h_{\mathrm{COMPR,in}}} \tag{2}$$

The COP_{h} takes into account the compressor isentropic efficiency, but not the mechanical, volumetric, and inverter efficiencies. The propagated measurement uncertainty in the COP_{h} was within 5%. For the performance assessment of heat pump cycles, the irreversible loss (de'Rossi et al., 1991) is calculated as follows. The total irreversible loss during cycling, L_{total}, can be divided into the following irreversible losses of the main elements (e.g., compressor and evaporator) and also the heat loss and pressure drop, as follows:

$$L_{\mathrm{total}} = L_{\mathrm{COND}} + L_{\mathrm{EVA}} + L_{\mathrm{EXP}} + L_{\mathrm{COMPR}} + L_{\mathrm{H}} + L_{\mathrm{P}} \tag{3}$$

Figure 2 illustrates irreversible losses generated in condenser, evaporator, expansion valve, compressor (departure from the isentropic compression), and connecting pipe in a *T-s* diagram. In the figure, water temperature and refrigerant temperature are plotted against the entropy generation rate. The irreversible losses per refrigerant mass in each component are calculated as follow,

$$L_{\mathrm{COND}} = \int_{s_{\mathrm{COND,in}}}^{s_{\mathrm{COND,out}}} \left(T_{\mathrm{R}} - T_{\mathrm{W}}\right) ds \tag{4}$$

$$L_{\mathrm{EVA}} = \int_{s_{\mathrm{EVA,in}}}^{s_{\mathrm{EVA,out}}} \left(T_{\mathrm{W}} - T_{\mathrm{R}}\right) ds \tag{5}$$

$$L_{\mathrm{EXP}} = \int_{s_{\mathrm{EXP,in}}}^{s_{\mathrm{EXP,out}}} T_{\mathrm{R}}\, ds \tag{6}$$

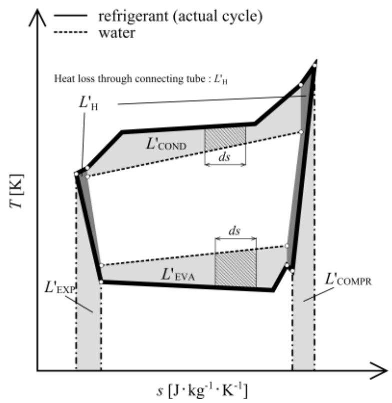

Figure 2: Irreversible loss in each element

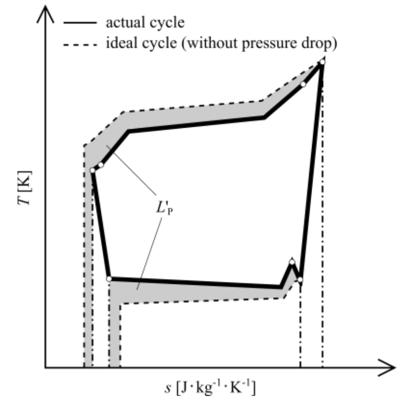

Figure 3: Irreversible loss by pressure drop

$$L_{\mathrm{COMPR}} = \int_{s_{\mathrm{COMPR,in}}}^{s_{\mathrm{COMPR,out}}} T_{\mathrm{R}}\, ds \tag{7}$$

Figure 3 illustrates the irreversible loss caused by pressure drop in a *T*-*s* diagram. The solid lines denote an actual cycle and the dashed lines denote an ideal cycle without pressure drop. The irreversible losses caused by pressure drop are expressed as hatched areas edged by the solid and dashed lines.

3. THERMODAINAMIC ANALYSIS METHOD

3.1 Calculation condition of thermodynamic analysis

Table 4 lists the analysis conditions at heating mode 1 and heating mode 2 that is the same as experimental condition. Efficiency of compressor is 1.0 to calculate ideal cycle. Calculated refrigerants are the same as experimental test refrigerants in table 3.

3.2 Calculation method of thermodynamic analysis

The calculations of type A and Type B are carried out. As shown in Figure 4(a), the calculation of type A is that

Table 4: Analysis conditions

	Heating mode 1	Heating mode 2
Heat source temperature [K]	288.15→ 282.15 (ΔT = 9 K)	
Heat sink temperature [K]	293.15→303.15 (ΔT = 10 K)	293.15→318.15 (ΔT = 25 K)
Degree of superheat [K]	3	
Heat transfer rate [kW] (Heating/cooling heat load)	2.2	
Efficiency of Compressor [-]	1.0	

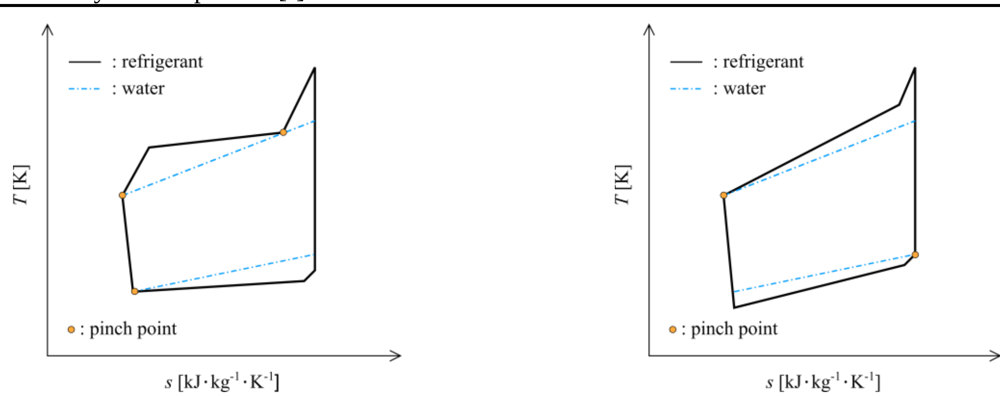

(a) type A (temp. glide is smaller) (b) type B (temp. glide is larger)

Figure 4: Calculation method of thermodynamic analysis

temperature glide of refrigerant is smaller than water temperature difference in the heat exchanger inlet and outlet. On the other hand, the calculation of type B is that temperature glide of refrigerant is larger as shown in Figure 4(b). The condensation and evaporation pressure is decided so that pinch points (temperature difference between refrigerant and water) become 0 K.

4. EXPERIMENTAL AND ANALYSIS RESULTS

4.1 Coefficient of performance (COP)

Figure 5 shows coefficient of performance for heating mode 1 and heating mode 2 in the experiment, where blue, red, green, purple and orange represent the results obtained for ternary 300, ternary 200, binary 300, binary 200 and R410A, respectively. The refrigerant charge is varied to find the maximum COP during the experiment. The optimized charge is determined as the refrigerant amount exhibits the highest COP at the most of conditions for each test refrigerant. The series of experimental data are obtained at that optimized refrigerant charge. For the heating mode 1, the *COP* of ternary300 and binery300 are comparable to that of R410A. The *COP* of ternary 200 and binary 200 are lower than that of R410A. For the heating mode 2, the *COP* trend due to differences in refrigerant is the same as that of heating mode 1. The difference in *COP* due to difference in refrigerant of heating mode 2 is,

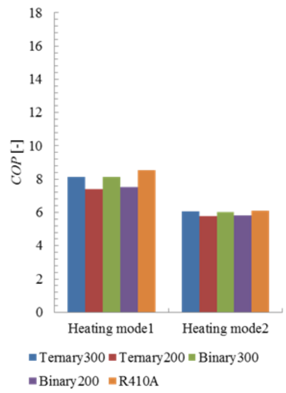

Figure 5: *COP* in the experiment

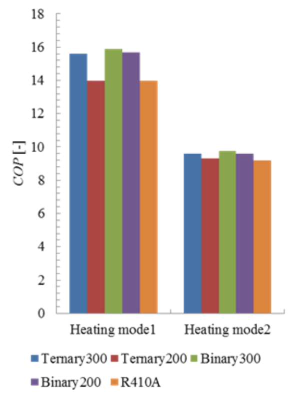

Figure 6: COP in the analysis

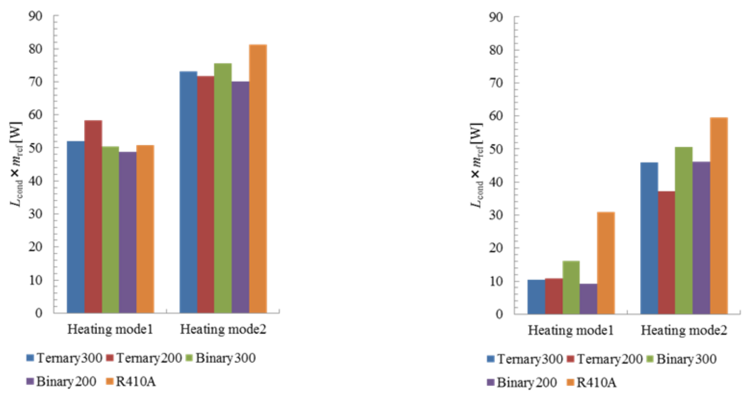

(a) Experimental result

(b) Analysis result

Figure 7: Irreversible loss in condenser

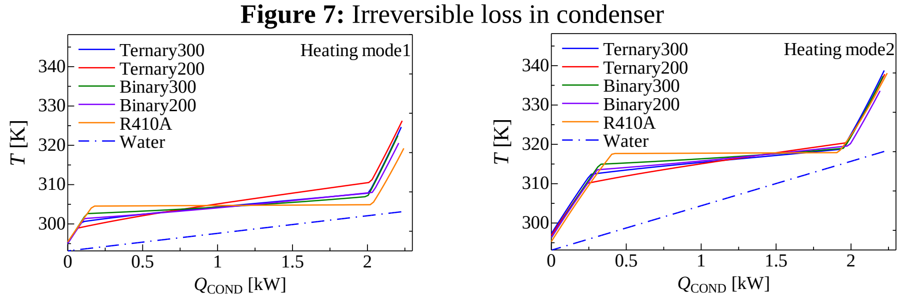

(a) heating mode 1

(b) heating mode 2

Figure 8: Temperature distribution in condenser in experiment

however, smaller than that of heating mode 1.

Figure 6 shows *COP* for heating mode 1 and heating mode 2 in the analysis. For heating mode 1, the *COP* of ternary 300, binary 300 and binary 200 are higher than that of R410A. For heating mode 2, the *COP* trend due to differences in refrigerant is the same as that of heating mode 1. The difference in *COP* due to difference in refrigerant of heating mode 2 is, however, smaller than that of heating mode 1. Compared with results in experiment and results in analysis, the *COP* trend due to differences in refrigerant in experiment differ from that in analysis.

4.2 Irreversible Loss of Condenser, Evaporator and Expansion Valve

Figure 7 (a) and (b) shows irreversible loss in condenser in experiment and analysis for heating mode 1 and heating mode 2. Symbols indicate the refrigerants in the same rule as in Figure 5. For heating mode 1, the irreversible loss in condenser of Ternary 200 is the largest among test refrigerants in experiment (Figure 7 (a)); the irreversible loss in condenser of R410A is, however, the largest among test refrigerants in analysis (Figure 7 (b). For heating mode 2, the trend of irreversible loss in condenser due to difference in refrigerant in experiment is the same as that in analysis.

The irreversible losses generated in condenser are determined by the mean temperature difference between refrigerant and heat sink water. Figure 8 (a) and (b) explains the temperature distribution in condenser for heating mode 1 and heating mode 2 in experiment. For heating mode 1, mean temperature difference between R410A and heat sink water is the smallest and mean temperature difference between Ternary 200 and heat sink water is the largest despite the temperature glide of Ternary 200 equal to water temperature change in the condenser. These causes are lower heat transfer coefficient of zeotropic mixture and lower heat transfer performance of heat exchanger. For heating mode 2, in all refrigerants, the temperature differences between refrigerant and heat sink water in condensing start point are much the same. Thus the trend of irreversible loss in condenser due to difference in refrigerant in experiment is the same as that in analysis.

Figure 9 (a) and (b) shows irreversible loss in evaporator in experiment and analysis for heating mode 1 and heating mode 2. Symbols indicate the refrigerants in the same rule as in Figure 5. Both in experiment results and analysis results, in all test refrigerants, the irreversible losses in evaporator for heating mode 1 are the same as that for heating mode 2. For heating mode 1 and heating mode 2, the trend of irreversible loss in condenser due to

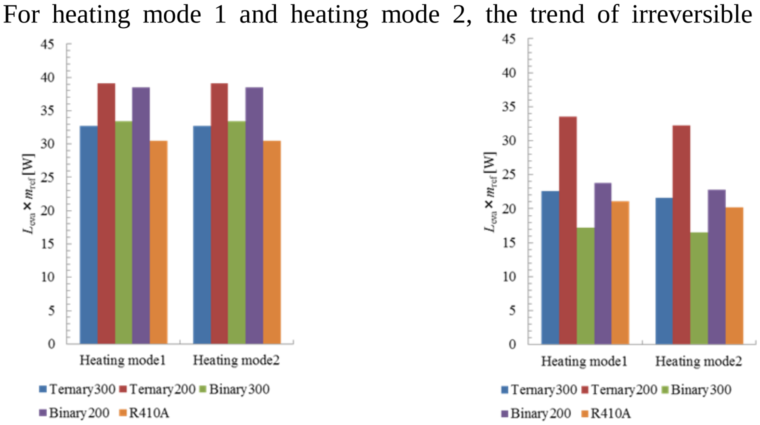

(a) Experimental result (b) Analysis result

Figure 9: Irreversible loss in evaporator

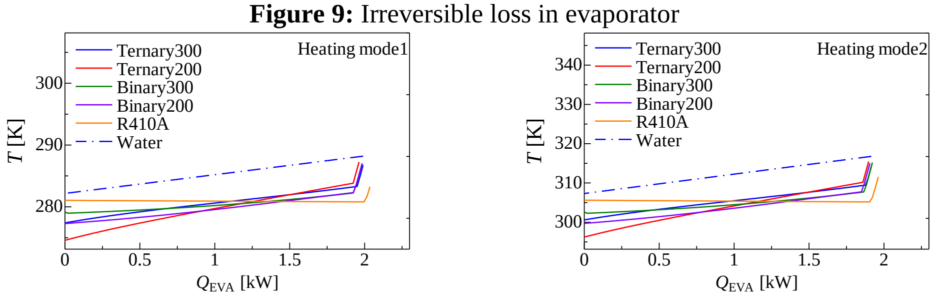

(a) heating mode 1 (b) heating mode 2

Figure 10: Temperature distribution in evaporator in experiment

difference in refrigerant in experiment is the same as that in analysis except irreversible loss in evaporator of Binary 300 in experiment is higher than another refrigerant.
The irreversible losses generated in evaporator are determined by the mean temperature difference between refrigerant and heat source water. Figure 10 (a) and (b) explains the temperature distribution in evaporator for heating mode 1 and heating mode 2 in experiment. The temperature distributions in evaporator for heating mode 1 are the same as that for heating mode 2 in all test refrigerants. For heating mode 1 and heating mode 2, temperature difference between Binary 300 and heat sink water is the largest among test refrigerant in evaporating end point despite the temperature glide of Binary 300 equal to water temperature change in the evaporator. Therefore, as results of irreversible loss in condenser and evaporator, even if temperature glide of zeotropic mixture equal to water temperature change in the heat exchanger, irreversible loss in heat exchanger increases because of lower heat transfer performance of heat exchanger.

Figure 11 (a) and (b) shows irreversible loss through expansion value in experiment and analysis for heating mode 1 and heating mode 2. Symbols indicate the refrigerants in the same rule as in Figure 5. For heating mode 1 and heating mode 2, the trend of irreversible loss through expansion valve due to difference in refrigerant in experiment is the same as that in analysis

4.3 Irreversible Loss of Compressor and Pressure Drop

Figure 12 shows irreversible loss in compressor in experiment for heating mode 1 and 2. On other hand, irreversible loss in compressor in analysis is not exist because efficiency of compressor is 1.0 in this analysis. For heating mode 1 and 2, the irreversible loss in compressor of R410 is the smallest among test refrigerants. At zeotropic mixture, the more the temperature glide is large, the more the irreversible loss in compressor is large. In other words, the more the thermophysical property of zeotropic mixture is different from that of R410A, the more the irreversible loss in compressor is large. This cause is that compressor and compressor oil in this study are compressor and compressor oil for R410A. Therefore, the irreversible loss in compressor of zeotropic mixture decreases if compressor is improved.

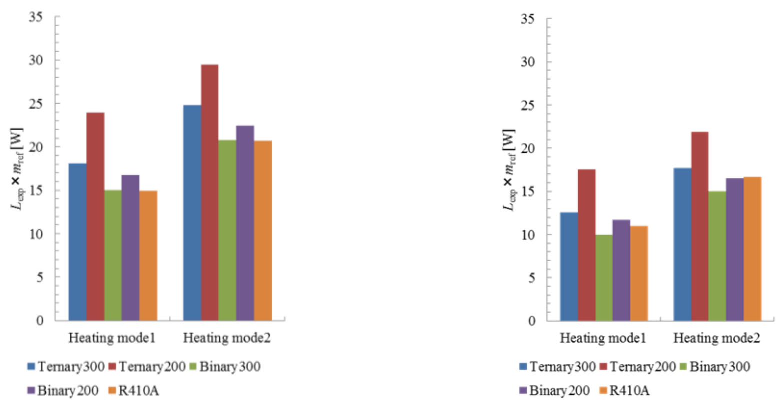

(a) Experimental result (b) Analysis result

Figure 11: Irreversible loss through expansion valve

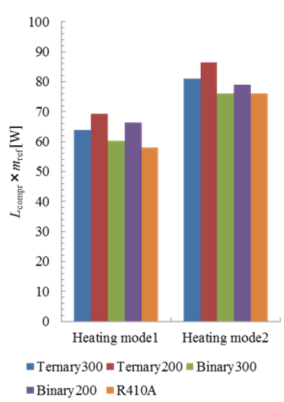

Figure 12: Irreversible loss in compressor

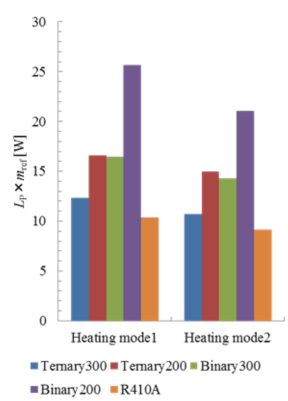

Figure 13: Irreversible loss caused by pressure drop

Figure 13 shows irreversible loss caused by pressure drop for heating mode 1 and 2. On other hand, irreversible loss caused by pressure drop in analysis is not exist because pressure drop is ignored in this analysis. For heating mode 1 and 2, the more the volumetric capacity is small, the more the irreversible loss caused by is large. Therefore, the irreversible loss caused by pressure drop decreases if the diameter of connecting pipe and heat exchanger is increased.

4. CONCLUSIONS

The *COP* of four test refrigerants, R410A, R32, R1234ze(E)/R32(20/80 mass%), and R1234ze(E)/R32 (50/50 mass%) has been experimentally and analytically evaluated with a heat pump cycle. The concluding remarks are as follows:

(1) For heating mode 1 and 2, in experiment, *COP* of Ternary 300 and Binary 300 are comparable to that of R410A. In analysis, *COP* of Ternary 300, Binary 300 and Binary 200 are higher than that of R410A

(2) Even if temperature glide of zeotropic mixture equal to water temperature change in the heat exchanger, irreversible loss in heat exchanger increases because of lower heat transfer performance of heat exchanger.

(3) *COP* of Ternary 300, Binary 300 and Binary 200 are higher than that of R410A in experiment if compressor is improved and the diameter of connecting pipe and heat exchanger is increased.

NOMENCLATURE

COP	coefficient of performance	(-)
h	enthalpy	$(kJ \cdot kg^{-1})$
L	irreversible loss	$(kJ \cdot kg^{-1})$
m	mass flow rate	$(kg \cdot s^{-1})$
Q	heat transfer rate	(kW)
T	temperature	(K)
s	entropy	$(kJ \cdot kg^{-1} \cdot K^{-1})$
W	compression work	(kW)

Subscripts

COND	condenser
COMPR	compressor
EVA	evaporator
EXP	expansion valve
H	heat loss
h	heating mode
in	inlet
R	refrigerant
out	outlet
P	presser drop

REFERENCES

de'Rossi, F., Mastrullo, R., Mazzei, P., (1991). Working fluids thermodynamic behavior for vapor compression cycles. *Appl. Energy*, 38, 163–180.

Jakobs, R., Kruse, H., (1978), The use of non-azeotropic refrigerant mixture in heat pumps for energy saving, *Proceeding of IIR Commissions B2, Delft*(207-218), Netherlands: IIR

Kojima, H., Fukuda, S., Kondou C., Takata, N., Koyama, S., (2015), Comparative assessment of heat pump cycle operated with R32/R1234ze(E) and R32/R1234yf mixtures, *Proceeding of The 24th IIR International Congress of Refrigeration, Yokohama* (1-8). Kanagawa, Japan: IIR

Kruse, H, (1981), The advantages of non-azeotropic refrigerant mixtures for heat pump application, *Proceeding of IIR Commissions D1, D2, E1, and E2*, (119-125): IIR

McLinden, M.O., Radermacher, R., (1987), Methods of comparing the performance of pure and mixed refrigerants in the vapour compression cycle, *Int. J. Refrig*., 10, 318-325.

Swinney, J., Jones, W.E., Wilson, J.A., (1998), The impact of mixed non-azeotropic working fluids on refrigeration system performance, *Int. J. Refrig*., 21(8), 607-616.